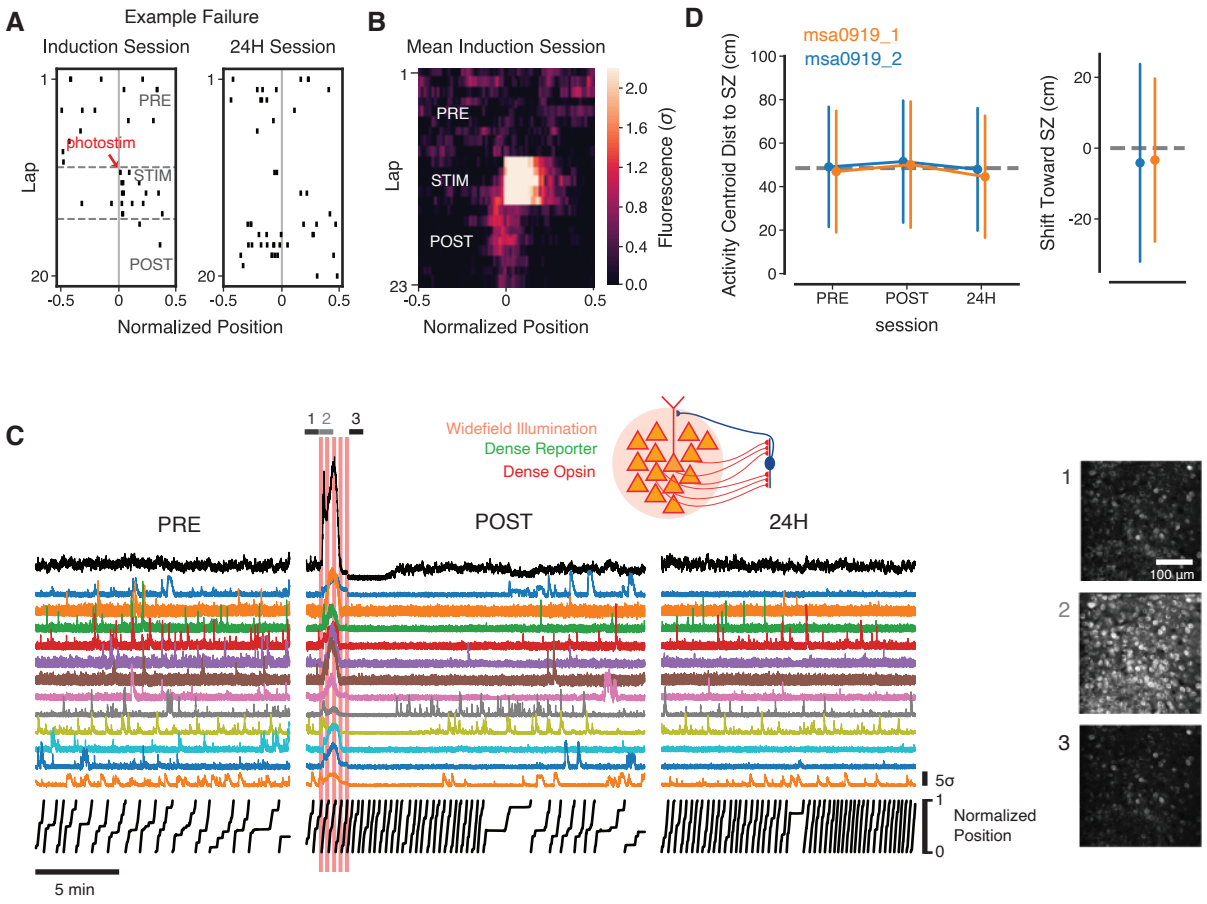

Figure S1. Widefield photostimulation of all CA1PCs leads to epileptiform-like activity without spatial overrepresentation of the SZ. (Related to Figure 1). **(A)** Raster of the running-related activity (deconvolved events) of an example cell in which opto-PFi failed. Induction session and 24H follow-up session shown as in Fig 1D. **(B)**Heatmap of fluorescence (z-scored) across all stimulated cells during induction sessions. **(C)** Calcium activity before, during, and after induction protocol in an example CaMKII-Cre mouse virally expressing $(\text{ChRmine})^{\text{Cre}}$ and $(\text{GCaMP6f})^{\text{Cre}}$ in all CA1PCs. *Top,* Schema of circuit during widefield optogenetic stimulation. Mean z-scored fluorescence activity (black, top) and activity of 12 example cells shown for each session with normalized position below. Red bars indicate photostimulation periods. *Bottom,* Normalized position of mouse over time on the treadmill belt; each black trace represents an individual lap. Note that mouse continues to run after photostimulation during the minutes-long, FOV-wide suppression of unit activity followed by slow recovery. *Right,* Time-averaged FOV during the numbered 1500 frame-long (∼50s) periods in POST session immediately before, during, and after photostimulation indicated at the top of **C**. **(D)** *Left,* Activity centroid distance from the stimulation zone for all cells in each of two mice during each session. *Right,* Shift toward the stimulation zone from PRE to POST for all cells. Data are represented as mean±sd.

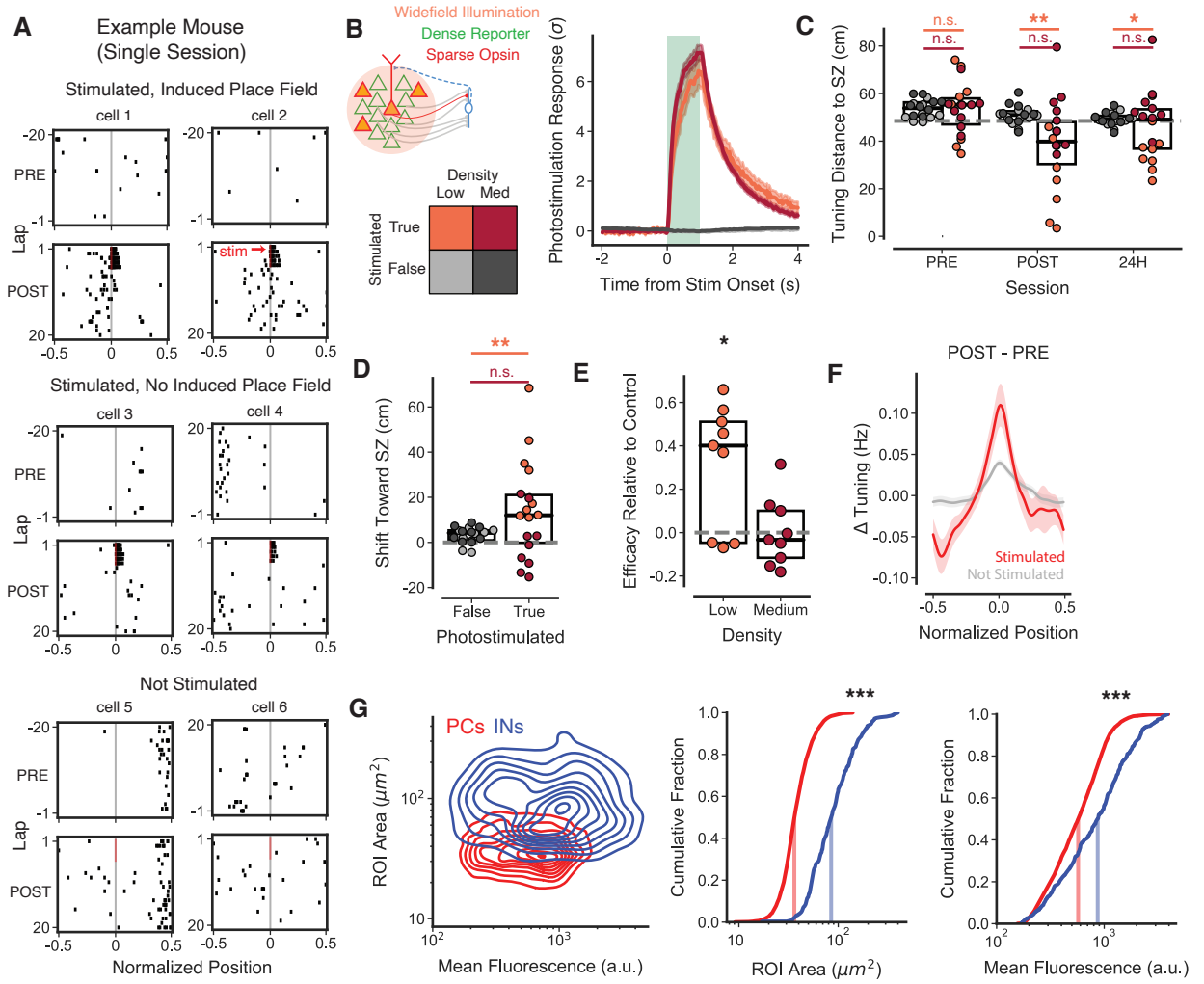

Figure S2. Unstimulated neighboring cells do not show peri-SZ activity bias and putative interneurons are clearly separable from CA1PCs based on morphology. (Related to Figure 2). **(A)** Raster of the running-related activity (deconvolved events) for example cells from a single widefield photostimulation induction experiment, including PRE and POST sessions. **(B)** *Left,* schema of circuit during widefield photostimulation of sparse CA1PC subpopulation. *Right,* mean z-scored fluorescence of cells in response to photostimulation. Green highlighting indicates photostimulation period. Data divided into Low and Medium Density experiments as in Fig 2C-E and grouped by cells showing photostimulation responses (Stimulated) vs. no response (Unstimulated; see *Methods*). Low Density Stimulated (orange): $n = 43$ cells, 9 mice; Low Density Unstimulated (light gray): $n = 2395$ cells, 9 mice; Medium Density Stimulated (rouge): $n = 204$ cells, 9 mice; Medium Density Unstimulated (dark gray): $n = 3245$ cells, 9 mice. **(C)** Mean tuning Distance to SZ for unstimulated and stimulated cells in each experiment ($n = 9$ mice for each group). **(D)** Mean activity centroid shift toward SZ from PRE to POST. **(E)** Difference in induction efficacy (i.e., fraction of cells with new place field near SZ during POST) for stimulated vs unstimulated cells in each experiment separated by density. In **C,D**, individual data points represent mean across cells for a single mouse FOV. For **C-E**, boxes indicate median and interquartile range for all points. Colors indicate density group as defined in **B** and Figure 2D. Asterisks indicate significant difference, colored by density group (paired Student's t-test, unstimulated vs. stimulated or one-sample Student's t-test against null hypothesis of 0 (**E**). **(F)** Change in tuning from PRE to POST for stimulated and unstimulated cells. Shading indicates mean±sem. Note the unstimulated population shows some increase in tuning near the SZ due to exclusion of peri-SZ PFs in PRE (see *Methods*). **(G)** *Left*, Distribution of mean time-averaged ROI fluorescence and surface area for PCs (red; $n = 4103$) in *s. pyramidale* and putative interneurons (blue; $n = 317$) in *s. oriens* in experiments shown in Fig 2I-K (6 mice). *Center*, cumulative distribution ROI sizes for PCs in *s. pyramidale* and putative interneurons in *s. oriens*. *Right*, cumulative distribution of ROI brightness for PCs and putative *s. oriens* interneurons. Vertical lines indicate median. Asterisks indicate difference via unpaired Student's t-test.

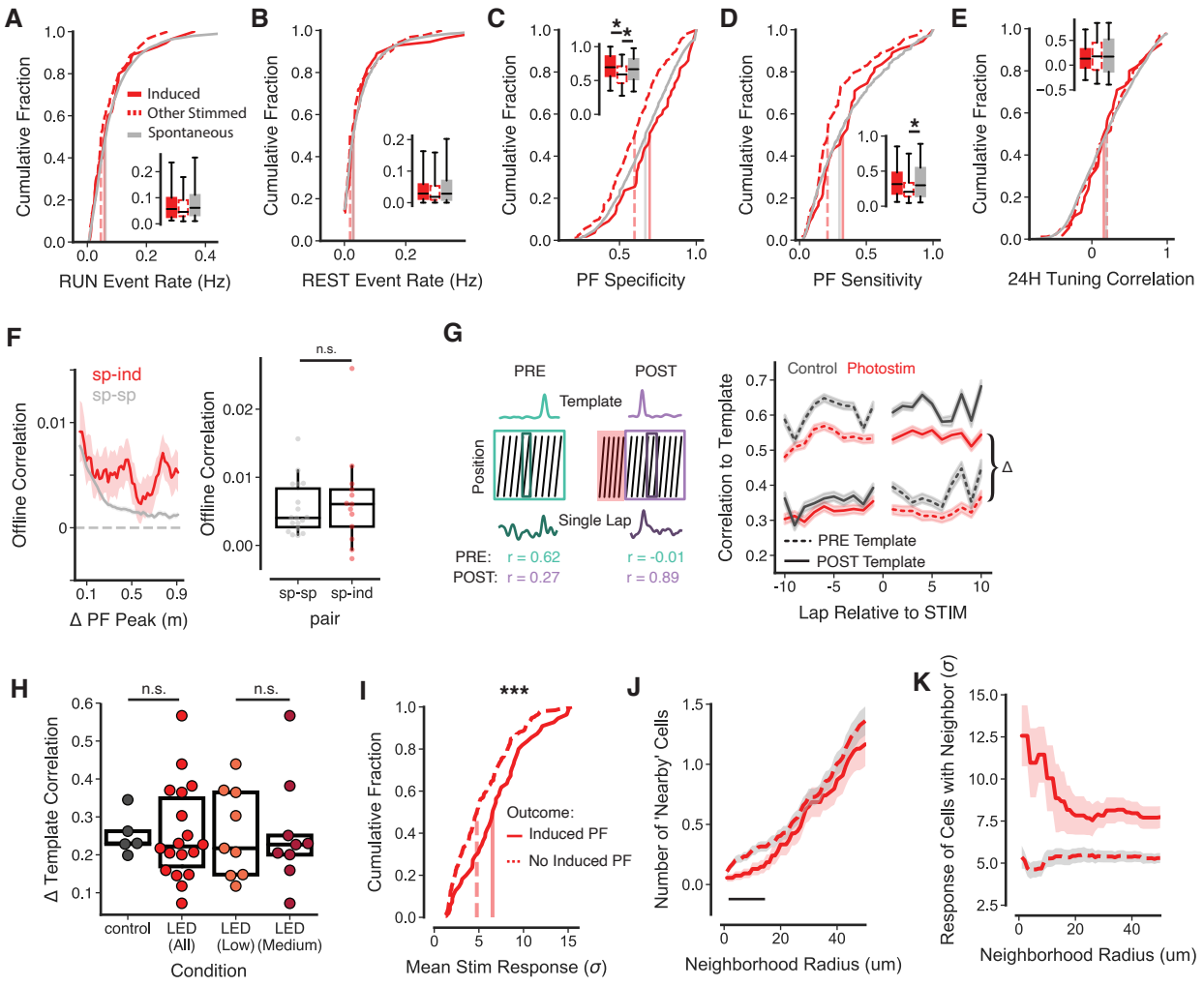

Figure S3. Characteristics of CA1PCs with PFs induced through opto-PFi. (Related to Figures 2 and 3). **(A)** Distribution of event rates during POST mobility for cells with induced PFs (solid red; $n = 55$), other photostimulated cells with spontaneous PFs away from the SZ (dashed red; $n = 85$), and unstimulated cells with spontaneous PFs (gray; $n = 3592$); $n = 18$ mice. **(B)** Distribution of event rates for POST immobility epochs. **(C)** Distribution of PF specificity (fraction mobility-related events occurring inside the PF). **(D)** Distribution of PF sensitivity (fraction PF traversals with detected events). **(E)** Distribution of 24h tuning stability (the Pearson's correlation between tuning curves from POST and 24H sessions). For **A-E,I**, vertical lines indicate median. Inset indicates interquartile range and 95% confidence interval for each group. Asterisks indicate $p < 0.05$ for Tukey's test after $p < 0.05$ for one-way ANOVA. **(F)** *Left*, pairwise signal correlations during immobility ('offline') between spontaneous-spontaneous (s-s, n=550594 pairs) and spontaneous-induced (s-i, n=22608 pairs) place cells, binned by pairwise PF peak distance in a sliding window of 4 spatial bins (7.76 cm). *Right*, mean across all pairs/distances by experiment. Difference between groups is not significant (independent Student's t-test, p=0.5544). **(G)** *Left,* schematic of template-based lap-by-lap remapping analysis. Note that PRE and POST are separated by a ∼20 min home cage rest period (Fig 2B). For each of the ten laps before (PRE) and after (POST) STIM, the correlation of a place cell's tuning on that lap to the mean tuning during either the PRE or POST session is computed. *Right,* Pearson's correlation of cells to PRE or POST templates for each lap around STIM. Data from photostimulation experiments (red) or opsin-negative controls (black). Note the large change (Δ) in correlations during POST (laps > 0) for both photostimulated and control mice, suggesting broad PF remapping at baseline (Fig 2B). **(H)** Difference in mean POST lap correlation from PRE template to POST template by experiment (Δ in **G**). Independent Student's t-test; control vs all: $p = 0.961$; low vs medium: $p = 0.973$. **(I)** Mean stimulation response amplitude for photostimulated cells with successful PF induction (solid; $n = 55$) vs other photostimulated cells (dashed; $n = 192$). Induced: 6.79±0.48; Non-induced: 5.36±0.22; $p = 0.0039$ independent Student's t-test. **(J)** Mean number of stimulated cells (regardless of whether they developed induced PFs or not) within a given radius for successfully induced vs other photostimulated cells. Black bar indicates $p < 0.05$ for independent Student's t-test at each 1 μm bin. **(K)** Mean stimulation response (z-scored fluorescence) for photostimulated cells with at least one photostimulated neighbor in the given radius. Shading indicates mean±sem.

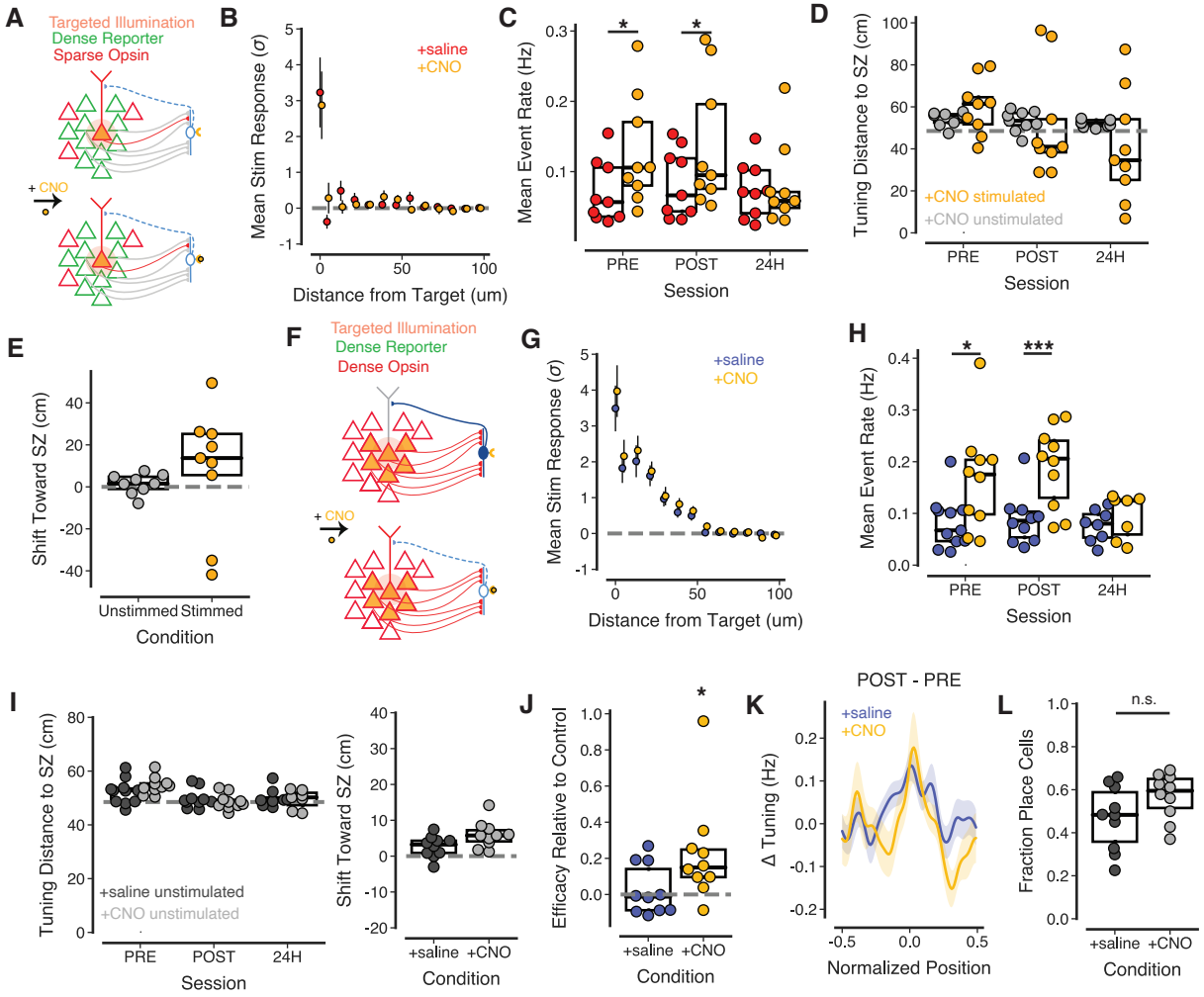

Figure S4. Suppression of inhibition enhances opto-PFi efficacy only during ensemble co-activation. (Related to Fig 3). **(A)** Schema of 2p targeted stimulation during sparse excitatory opsin expression as in Fig 3A-E. Relates to panels **B-E**. **(B)** Photostimulation response is local to targeted cell in sparse preparation with or without GiDREADD-mediated suppression of local interneuron activity with CNO. +saline: $n = 1750$ cells, +CNO: $n = 1785$ cells. Bars indicate mean±sem. Independent Student's t-test between groups, $p > 0.05$ for all bins. **(C)** CNO administration indirectly increases event rates for unstimulated PCs during PRE and POST, but effect washes out by 24h. Asterisks for one-sided paired Student's t-test. $n = 9$ mice. **(D)** Activity centroid distance to SZ for stimulated and unstimulated cells in +CNO condition (compare to Fig 3D). **(E)** Shift toward SZ for stimulated and unstimulated cells in +CNO condition (compare to Fig 3D). **(F)** Schema of 2p targeted photostimulation during dense excitatory opsin expression as in Fig 3F-I. Relates to panels **G-K**. **(G)** Same as **B** but for dense opsin expression. Photostimulation response spreads to ∼50μm around targeted cell in both conditions. +saline: $n = 2369$ cells, 5 mice; +CNO: $n = 2230$ cells, 4 mice. **(H)** Same as **C**. **(I)** Activity centroid distance to SZ (*Left*) and shift toward SZ from PRE to POST (*Right*) for unstimulated cells in each condition. Compare to Fig 3G,I. **(J)** Difference in efficacy (Fraction of cells with peri-SZ PF formation) for stimulated cells and unstimulated cells in each condition. Induction efficacy is higher than unstimulated control peri-SZ PF formation rate only after interneuron suppression. mean±sem; +saline: 0.0240±0.0443; +CNO: 0.2240±0.0902. One-sample Student's t-test against null hypothesis of 0: +saline: $p = 0.6015$; +CNO: $p = 0.0350$. **K** Change in tuning from PRE to POST for stimulated cells. Shading indicates mean±sem. **(L)** Fraction of place cells in the unstimulated population is not changed by CNO administration. Independent Student's t-test: $p = 0.0710$.